

# Hand-held percussion machines with low emission of hazardous vibration

I.J. Sokolov, V.I. Babitsky\*, N.A. Halliwell

*Wolfson School of Mechanical and Manufacturing Engineering, Loughborough University, Leicestershire, LE11 3TU, UK*

Received 7 November 2006; received in revised form 22 May 2007; accepted 24 May 2007

---

## Abstract

Vibration and impacts are essential features of many domestic and industrial hand-held machines. In many machines vibration cannot be avoided because of the vibro-impact nature of the working process. The only way to minimise an operator's exposure to harmful vibration in this case is to design the machine rationally. In this paper a percussion machine is considered as a multi-body vibro-impact system. The simplest structures have been found and investigated in which a strong vibro-impact process can be obtained with one body (casing/handle) being free of vibration. Computer simulations using Matlab-Simulink software and initial experiments validate the new approach. The main feature of the proposed new design is the use of a mechanism with zero differential stiffness. A hydro-pneumatic unit with zero stiffness was developed and tested. The new engineering solution was applied to a hydraulic breaker. Even a partial modification of the existing design and effective use of existing hydraulic power source demonstrated a significant improvement in performance.

© 2007 Elsevier Ltd. All rights reserved.

---

## 1. Introduction

Vibration and impacts are essential features of many domestic and industrial hand-held machines. In machines such as hammer drills, breakers, chipping hammers and similar, vibration cannot be avoided because of the vibro-impact nature of the working process. The only way to minimise the operator's exposure to harmful vibration is to improve the machine's design. Different approaches can be used including:

- reduction of intensity of the source of vibration,
- vibration isolation,
- dynamic absorption.

Partial reduction in the intensity of the source of vibration can be achieved in many machines by reduction in the excitation force amplitude via optimising the waveform of the alternating force. However, if the vibro-impact regime is an essential feature of the working process, this way of the vibration reduction has natural limitations because of the prescribed intensity of the vibro-impact regime. The general solution for the optimal

---

\*Corresponding author. Tel.: +44 0 1509 227503; fax: +44 0 1509 227502.

E-mail address: [V.I.Babitsky@lboro.ac.uk](mailto:V.I.Babitsky@lboro.ac.uk) (V.I. Babitsky).

excitation waveform has been found in Ref. [1] as a result of consideration of the equivalent problem of optimal control.

This paper is aimed at the synthesis of the structures of percussion machines with low emission of hazardous vibration. The best machine combines both optimal structure and excitation. The optimal excitation is used to compare different designs considered in the paper.

The optimal periodic excitation force  $u(t)$  with minimum amplitude  $\min_u \max_{t \in [0, T]} |u(t)|$  was found in Ref. [1] for the system shown in Fig. 1a with a prescribed period of vibration  $T$ , impact velocity  $v_0$  of the striker 1 and a single impact during the period.

The optimal excitation is shown in Fig. 1b. Here  $t$  is time,  $t_1$  is the time interval (part of the period  $T$ ) when the excitation force  $u(t)$  is positive and  $U_0$  is the amplitude of the excitation force. The time interval  $t_1$  and amplitude  $U_0$  are defined by [1]:

$$\frac{t_1}{T} = \frac{1}{1+R} \left( 1 - \sqrt{1 - \frac{1-R^2}{2}} \right), \quad U_0 = \frac{M_1(1+R)^2 v_0}{2T(\sqrt{1 - 0.5(1-R^2)} - 0.5(1-R))}, \quad (1)$$

where  $R = -v_+/v_0$  indicates the change of the absolute velocity of the striker (Item 1 in Fig. 1a) during impact,  $v_+$  is its upward velocity after impact and  $M_1$  is the mass of the striker. Hereafter positive values of the force applied to the striker and positive displacements correspond to the upward direction along the machine axis.

The force of excitation  $u(t)$  is applied to both the striker and the casing (Item 2 in Fig. 1a). If the friction between these two bodies and the friction between the tool (Item 3 in Fig. 1a) and the casing are negligibly small, the excitation force  $u(t)$  is the only source of the casing vibration. The optimal excitation was found for a system without friction.

In what follows we refer to the media being treated (Item 4 in Fig. 1a) as *ground*; in all figures constant forces are shown with solid line arrows, alternating forces are shown with dashed line arrows and the sequence of impact impulses is shown with dotted line arrows.

The force of excitation  $u(t)$  has a constant component  $\bar{u}$  and an alternating component  $\tilde{u}$  given by equations [1]:

$$\begin{aligned} \bar{u} &= -M_1 f (1+R) v_0, \\ \tilde{u}(t) &= u(t) - \bar{u}. \end{aligned} \quad (2)$$

Here  $f = 1/T$  is the frequency of impacts.

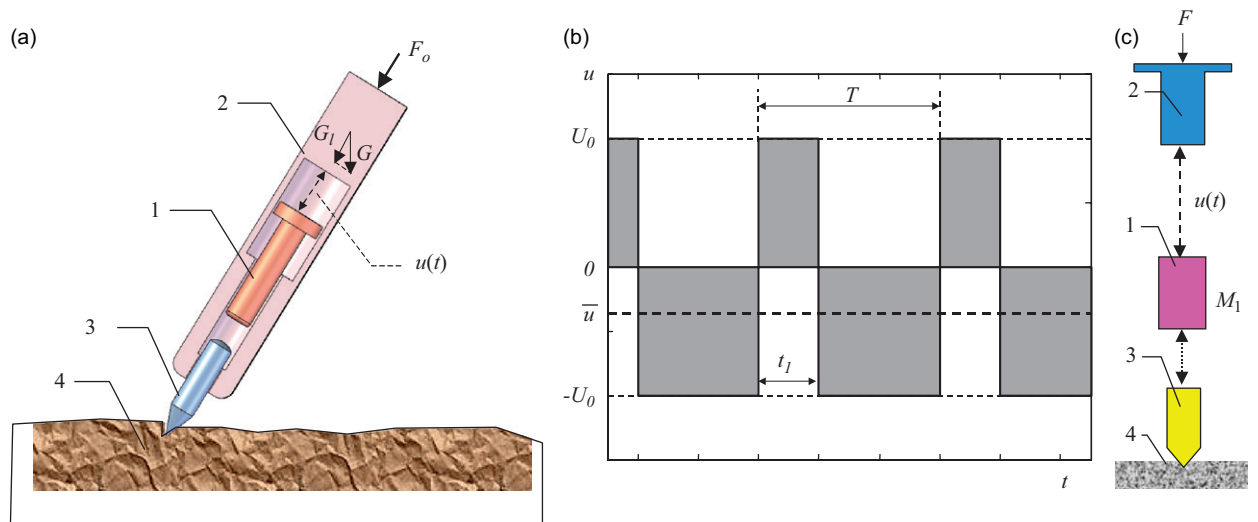


Fig. 1. Optimal excitation with minimum amplitude.

The constant component  $\bar{u}$  depends only on the parameters  $M_1$ ,  $R$ , of the system and the parameters  $T$ ,  $v_0$  of the regime. This component remains the same for any other excitation that provides the same parameters  $T$ ,  $v_0$  of the vibro-impact regime with a single impact per period. For example, other criteria can be used to optimise the force of excitation. The optimal excitation with minimal root-mean square (rms) can be also found in the cited paper [1]. It has the same constant component (2) as the optimal excitation with minimum amplitude (1). This is because the first equation in Eq. (2) follows from the impulse-momentum principle for external forces applied to the machine.

As a result, for the system with parameters  $M_1$  and  $R$  the desired vibro-impact regime of operation with parameters  $T$  and  $v_0$  is available only if the operator is able to apply a constant feed force  $F_0$  that together with the longitudinal component  $G_l$  of the casing weight  $G$  balances the constant component  $\bar{u}$  of the excitation force, i.e.

$$|\bar{u}| = G_l + F_0 = F. \quad (3)$$

Here  $F$  is the full feed force. For simplicity we will not distinguish the operator's feed force from the full feed force. However, it is important to note that the latter force has the casing weight component that depends on the breaker orientation. In what follows when the short term *feed force* is used it refers to the full feed force. According to Eq. (2), for any excitation that provides a vibro-impact regime with impact velocity  $v_0$  and single impact during a period  $T$  the full feed force can be found as

$$F = \frac{M_1(1+R)v_0}{T} = M_1(1+R)v_0f. \quad (4)$$

For the optimal excitation shown in Fig. 1b:

$$F = \left(1 - \frac{2t_1}{T}\right)U_0. \quad (5)$$

The equivalent structure of such a system with negligibly small friction is shown in Fig. 1c. For this system a reduction in harmful vibration transmitted to an operator can only be achieved by increasing the casing mass or by adding extra inertial bodies. Increasing the mass of the casing is a very straightforward solution with obvious disadvantages. This approach is described in Ref. [2] where the mass of the breaker is increased and decreased rapidly by transferring fluid from an external reservoir to the hollow casing of the breaker each time the breaker is switched on and back to the reservoir each time the breaker is switched off. This enables an operator to move the breaker manually when it is switched off. Although this solution does allow for reduction in the breaker casing vibration, it produces a more bulky breaker with an external reservoir and a power pack with a high volume flow rate needed to move large volumes of liquid rapidly.

In this paper, other means of improving the design of hand-held percussion machines are investigated. The aim is to reduce significantly the operator's exposure to the hazardous vibration for prescribed intensity of the vibro-impact working process, but without increase in the machine's mass. The structures of machines with the vibration-free handle are synthesised and validated.

In this aspect the first approach is to change the design so that the reaction force of the alternating component of the excitation is applied not to the casing, but to the ground. This can dramatically reduce vibration of the casing and is analysed thoroughly in the next section.

## 2. Optimal solution for three-body system

The simplest and the most obvious way to reduce the emission of harmful vibration is shown in Fig. 2a. This system is almost identical to the one shown in Fig. 1a and c. However, the casing 2 is now pushed onto the ground 4 by the constant feed force  $F_1$  provided by the operator. If the feed force exceeds the amplitude  $U_0$  of the excitation force  $u(t)$  the alternating component of the excitation force is fully balanced by the force  $N$  of the ground reaction:

$$F_1 > U_0 \Rightarrow N(t) = F_1 - u(t) > 0. \quad (6)$$

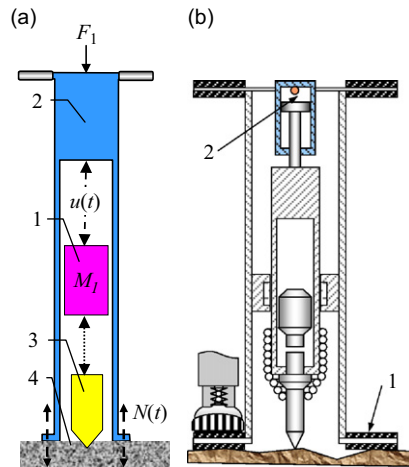


Fig. 2. Simplest three-body system with zero vibration.

A positive sign of the alternating force  $N(t)$  means that the casing does not ‘jump’ and hence its vibration is very low. Actually, the casing vibration for this scheme results only from the contact deformation of the ground under the alternating component  $\tilde{u}(t)$  of the excitation force. In practice this vibration would be usually negligibly low because of the high contact stiffness of the ground.

A low casing vibration is the only advantage of this scheme. It has, however, at least two serious disadvantages. Firstly, this machine is less convenient to handle and has a more limited range of application when compared with common hand-held and mounted percussion machines, which contact the ground only at the point of demolition. The other disadvantage is the necessity for a higher feed force  $F_1$ . For the optimal excitation (1):

$$\frac{F_1}{F} > \frac{1}{1 - (2t_1/T)}. \quad (7)$$

Here  $F$  is the feed force (5) for the initial system (Fig. 1c).

As a result of these disadvantages the scheme has not found a wide application. The authors do not know any examples of industrial application of such a scheme to percussion machines. However, a similar solution for a pneumatic tool has been patented in 1987 [3] and is shown schematically in Fig. 2b. This design has footplates 1 mounted to the casing, which help the operator to provide the higher feed force needed. It also has an extra body and a pneumatic cylinder 2 that allows for sizeable penetration of the tool into the ground without deterioration of the working vibro-impact process. The latter can happen in the self-sustained system with the excitation force controlled by the relative position of the striker 1 with respect to the casing 2 (Fig. 2a).

There is, however, another means of developing the initial system shown in Fig. 1c which provides a reduction in the casing vibration, but with fewer disadvantages. For the same structure with the same number of bodies, changing the way the excitation force is applied can dramatically reduce the casing vibration.

This can be achieved by separating the excitation force into two components  $u(t) = u_c + u_p(t)$ , as Fig. 3a shows.

The advantage of this separation is that the alternating (pulsating) component  $u_p(t)$  of the excitation force applied to the striker is now unidirectional and upward. As a result, this component can be applied between the striker 1 and the tool 3. In this case the unidirectional downward counterforce of this component of the excitation force is applied directly to the ground 4 (via the tool 3) as Fig. 3c shows. The constant component  $u_c$  can be applied between the striker 1 and the casing 2. The only force applied to the casing now is the constant component of the excitation force. This component can be balanced by the constant feed force  $F_2$ . As a result, this mechanical system can theoretically have a strong vibro-impact process on the one (lower) side and total absence of vibration on the other (upper) side. This is the optimal three-body system with minimal emission of

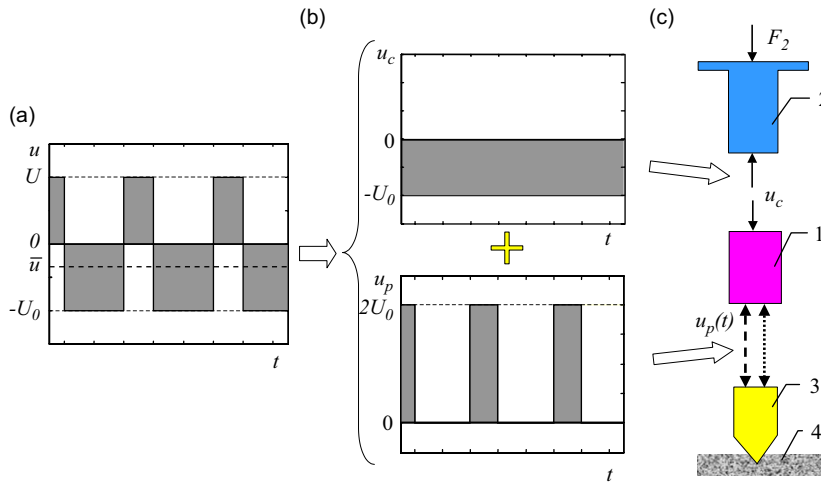


Fig. 3. Splitting excitation force into two components.

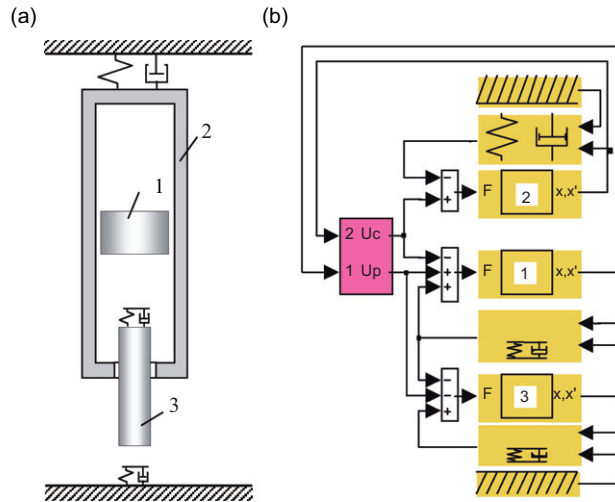


Fig. 4. Mechanical structure and Matlab-Simulink model of three-body system.

harmful vibration. It is important that the excitation (1) with minimal amplitude  $U_0$  is optimal in the new system as well because it minimises the feed force  $F_2 = |u_c| = U_0$ .

The existence of the solution with zero vibration of the casing has the following mechanical explanation: the pulsating component  $u_p(t)$  is needed only to compensate for the loss of the striker energy during impact. In the case of a very massive tool 3 and a theoretically ideal impact, without loss of energy, the pulsating component  $u_p(t)$  vanishes and the system is similar to a simple one-body mechanical model of the free bouncing ball in a gravity field. This simple analogy is given here only to help with understanding the fact that generally a vibro-impact machine can be designed with a vibration-free casing. The three-body system under consideration with two vibrating bodies and non-ideal impacts is more complex. However, stable vibro-impact regimes, with the parameters specified above, can be obtained in such a system and this has been confirmed by numerical simulations.

The mechanical structure shown in Fig. 4a was used for the computer model development. This is a multi-body mechanical system with nonlinear (impact) interaction of moving parts. Linear differential equations were used to describe the continuous motion of free bodies between impacts or without impacts.

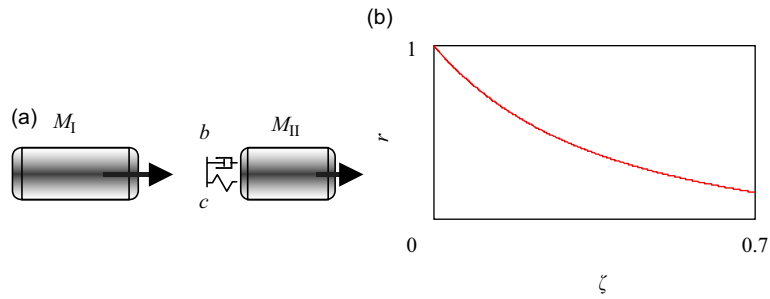


Fig. 5. Visco-elastic model of impact.

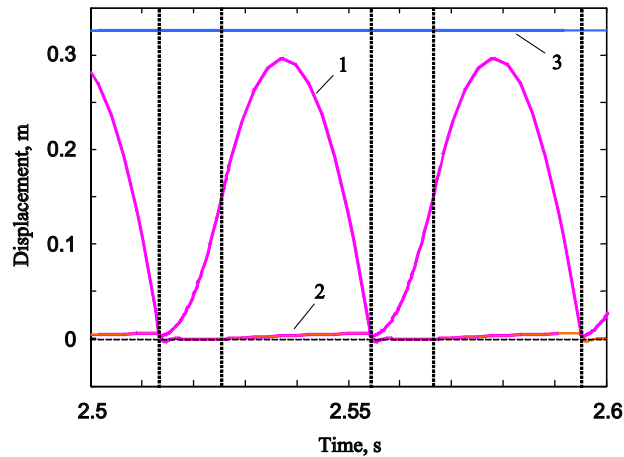


Fig. 6. Steady-state waveforms for three-body system.

Computational difficulties related to discontinuity of some variables during impacts can be avoided by using a Kelvin–Voigt model of a visco-elastic contact interaction of colliding bodies as introduced in Refs. [4,5]. This approach is able to describe impacts with different coefficients of restitution that depend on the properties of the colliding bodies. When using this model for any two bodies with masses  $M_I$  and  $M_{II}$  (Fig. 5a) the coefficient of restitution  $r$  depends on parameters in the following way [4,5]:

$$r(\zeta) = e^{-\zeta \tau(\zeta)} \frac{\sin\left(\sqrt{1-\zeta^2} \tau(\zeta)\right)}{2\zeta}, \quad \tau(\zeta) = \frac{\pi - a \tan \frac{2\zeta \sqrt{1-\zeta^2}}{1-2\zeta^2}}{\sqrt{1-\zeta^2}}. \quad (8)$$

Here

$$\zeta = \frac{b}{2\sqrt{c(M_I M_{II}/(M_I + M_{II}))}}$$

is the dimensionless damping;  $c$  is the contact stiffness coefficient;  $b$  is the contact damping coefficient.

Fig. 5b shows the function  $r(\zeta)$  defined by Eq. (8). It can be used to choose parameters  $b$  and  $c$  of the model for every pair of colliding bodies with known masses and coefficient of restitution.

Fig. 4b presents the corresponding aggregated Matlab–Simulink model of the three-body system. Fig. 6 shows an example of the resulting steady-state waveforms of the three-body system motion simulation. Solid lines show displacement of the bodies in meters; dotted lines show excitation force  $u_p(t)$  switching instants (see Fig. 3a).

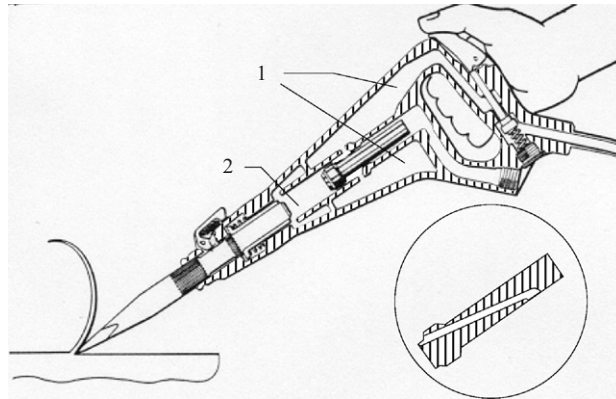


Fig. 7. Atlas Copco pneumatic chipping hammer.

The results were obtained for the following parameters:  $M_1 = 1$  kg,  $M_2 = 3$  kg,  $U_0 = 2050$  N and the following coefficients of restitution of colliding bodies:  $r_{12} = 0.3$  for striker/tool,  $r_{24} = 0.15$  for tool/ground. The values of  $M_1$  and  $M_2$  are close to typical ones for an industrial hydraulic heavy hand-held breaker. Amplitude  $U_0$  provides the frequency of vibration close to a typical one near 20 Hz. The model shown in Fig. 4b corresponds to a self-sustained oscillation system in which the excitation force is controlled by the relative position of the striker 1 and the casing 2. Stable regimes similar to those shown in Fig. 6 were obtained for systems with other parameters.

We found an example of an industrial application of the approach shown in Fig. 3. Atlas Copco corporation used this scheme for the development of a hand-held pneumatic chipping hammer RRD-36 [6,7] shown in Fig. 7.

This hammer has a differential piston. Air pressure on the smaller rear annular area of the piston (chamber 1) is constant. A special duct in the piston provides a pulsating pressure on the bigger front area (chamber 2). According to Atlas Copco, the vibration level of this hammer was reduced by 90% compared to conventional chipping hammers.

To the authors' knowledge there have been no further examples of the industrial application of this approach. This can possibly be explained by the fact that such a design still has one of the disadvantages intrinsic to the scheme shown in Fig. 2a. The feed force  $F_2$  for the new design is the same as the minimal feed force  $F_1$  (7) for the former system:  $F_2 = U_0$ . Although the new design is more convenient to use by an operator as compared to the one shown in Fig. 2, it has the same disadvantage: a higher operator's feed force  $F_2$  is needed for its operation, as compared to the feed force  $F$  for the traditional system (Fig. 1):

$$\frac{F_2}{F} = \frac{1}{1 - (2t_1/T)} > 1. \quad (9)$$

As was mentioned above, the optimal excitation with minimal amplitude (1) is optimal again in the new system as in this case it minimises the feed force. However, if, for example,  $t_1/T = 1/3$  the feed force needed for a vibration-free tool is three times as much as for the initial design (Fig. 1). To investigate this disadvantage more closely and in absolute terms we can rewrite Eq. (9) using Eqs. (4) and (1):

$$F_2 = \rho M_1 v_0 f, \quad \rho = \frac{1 + R}{1 - (2/(1 + R)) \left( 1 - \sqrt{1 - ((1 - R^2)/2)} \right)}. \quad (10)$$

The same impact energy  $E_0 = M_1 v_0^2 / 2$  can be achieved with different combinations of mass  $M_1$  and velocity  $v_0$ . For a prescribed energy and frequency of impacts, increasing the impact velocity  $v_0$  and reducing the mass  $M_1$  allows for a decrease in the excitation force. To reduce the number of variable parameters in expression (10) we will take a typical value of impact velocity of  $v_0 = 10$  m s<sup>-1</sup>, which is close to the maximum one used in industrial machines. Higher velocities usually cause fast deterioration of the of the striker/tool contact surfaces.

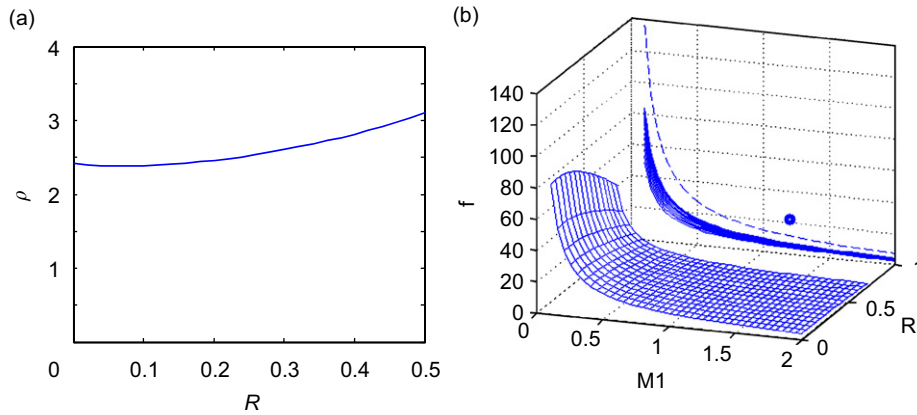


Fig. 8. Feasible parameters of three-body machine.

For  $0 < R < 0.5$  the parameter  $\rho$  depends very weakly on the coefficient  $R$  as Fig. 8a shows.

For  $v_0 = \text{const}$  and  $F_2 = \text{const}$  the expression  $\rho M_1 f = F_2 / v_0 = \text{const}$  describes a 3D surface that corresponds to possible combinations of the parameters  $R$ ,  $M_1$ ,  $f$  of the vibro-impact machine for a prescribed feed force  $F_2$  and impact velocity  $v_0$ . Typical value of the feed force  $F_2$  for this kind of machines is 150 N. Fig. 8b shows the surface plotted for  $F_2 = 200$  N and  $v_0 = 10 \text{ m s}^{-1}$ . Points lying above the surface relate to parameters that need a feed force in excess of 200 N.

This figure also shows the projection of the surface onto the vertical plane  $(M_1, f)$ . The bold circle in this plane presents typical parameters  $M_1 = 1.2 \text{ kg}$  and  $f = 22 \text{ Hz}$  of a heavy hand-held hydraulic breaker. It is therefore clear that such parameters cannot be achieved with a feed force of 200 N. Even in a vertical working position when the whole weight of the breaker casing is added to the operator's feed force this is still not sufficient as the dashed line shows. This line is plotted in the same vertical plane for  $F_2 = 350$  N and  $R = 0.25$ .

This analysis demonstrates that the approach shown in Fig. 3 can be applied only to light hand-held tools with a small striker mass or to mounted tools for which the operator's feed force is not so important.

In what follows we show that the introduction of an extra inertial body allows for a further theoretical solution of the problem of low vibration emission without the necessity for increasing the operator's feed force.

### 3. Optimal solution for four-body system

In the system shown in Fig. 9a the striker 1 is subjected again to a sequence of upward impact impulses. These impulses are balanced by the excitation force  $u(t)$  with the constant downward component  $\bar{u}$ . Inevitably, the excitation force  $u(t)$  has an alternating component to provide the periodic vibro-impact motion of the striker. The excitation force  $u(t)$  is applied between the striker 1 and the inertial body 2. Unlike the striker, the latter body can be balanced on average by a downward constant force  $u_c = \bar{u}$ , but it still vibrates. The inertia force resulting from this vibration balances the alternating component of the excitation force. For this reason hereafter we conventionally call this body a 'balance body'. The constant force is applied in this system between the balance body 2 and the body 5. The latter can be balanced by a constant feed force  $F_3$  and can carry a vibration-free handle. This is the optimal four-body system with minimum emission of harmful vibration and minimum operator's feed force  $F_3 = F = |\bar{u}|$ . In theory this scheme can be developed into two designs shown in Fig. 9b and c. Each of these modifications has both advantages and disadvantages. The main advantage of the former design is that the tool 3 is the only external part that vibrates in a steady-state regime, while the whole casing 5 does not vibrate. However, this design needs more complex arrangements to provide the alternating excitation force between bodies 1 and 2, both moving inside the motionless casing. The latter design is simpler; although only the handle 5 is free of vibration, while two other external parts (the casing 2 and the tool 3) vibrate.

Fig. 10a shows an aggregated Matlab–Simulink model corresponding to the system under review.



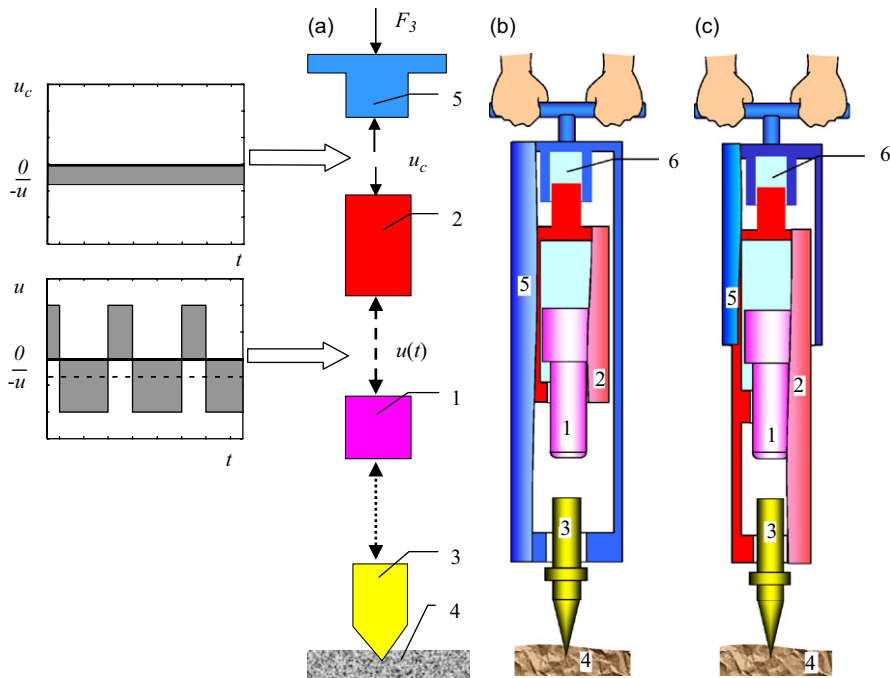


Fig. 9. Four-body system.

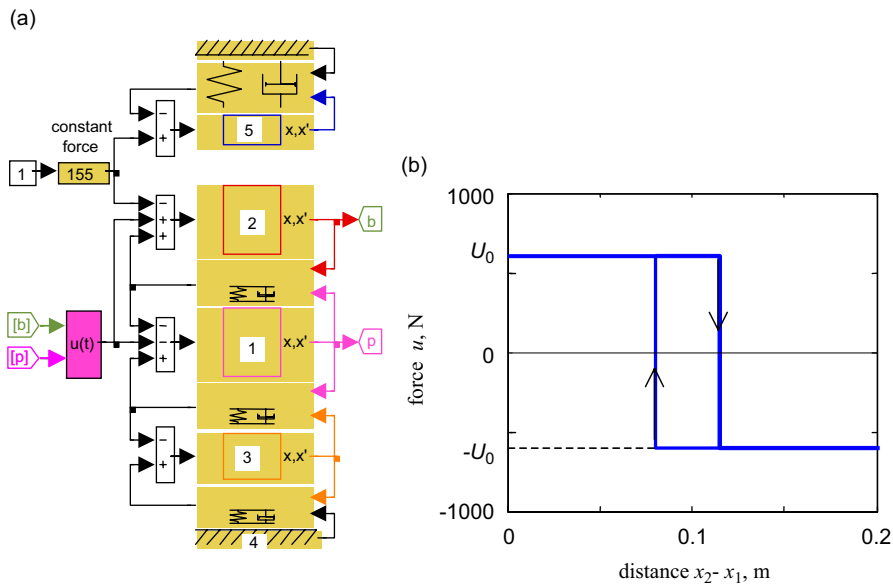


Fig. 10. Model of four-body system.

In this self-sustained system the excitation force  $u(t)$  is controlled by the relative position  $x_2 - x_1$  of the striker 1 and the balance body 2. The simplest relay law of control with  $U_0 = 600$  N was used as shown in Fig. 10b. Such excitation is very close to the one used in real hydraulic and pneumatic percussion machines.

Fig. 11a presents an example of the resulting transient process and the stable steady-state regime of vibration of the four-body system; curve numbers correspond to the numbers of the bodies in Fig. 9a. Fig. 11b

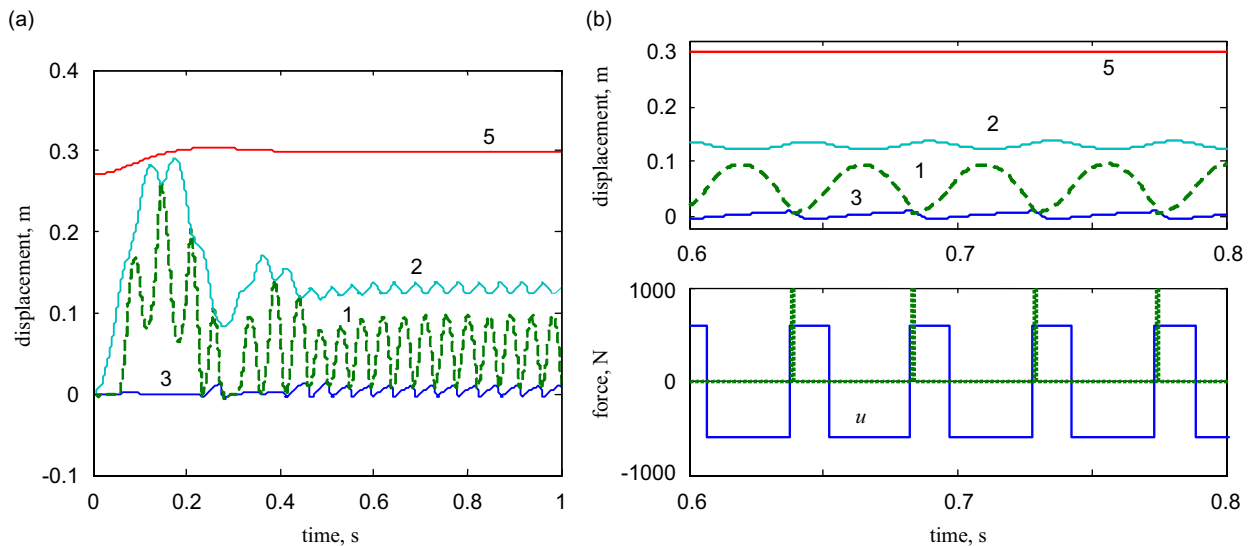


Fig. 11. Transient process and steady-state regime of four-body system.

shows the steady-state regime in more detail (upper diagram) along with the excitation force  $u$  and impact force between the striker and the tool (lower diagram). Impact instants in the latter diagram are shown with the dotted line. These results were obtained for the following parameters:  $M_1 = 1.2$ ,  $M_2 = 5$ ,  $M_3 = 3.5$ , and  $M_5 = 10$  kg,  $r_{12} = 0.25$ ,  $r_{24} = 0.15$ ,  $F_3 = 155$  N. The simulation has shown that the desired stable periodic regimes of vibration with single impact during a period of vibration can be obtained in a four-body system with a vibration-free handle. It is important that these regimes have low sensitivity to the system parameters deviation.

#### 4. Zero-stiffness suspension

Both designs shown in Fig. 9b and c feature some ideal element 6 that provides a constant force of interaction between bodies 2 and 5. The structure in Fig. 9c is in fact a very particular case of the common one of a percussion machine with the vibro-isolated handle. The main advantage of the new system—vibration-free handle—is a result of the fact that the new ideal suspension ensures constant force and hence it has zero differential stiffness in contrast to a common design with a spring-suspended handle [8].

Generally, a vibration isolator can be considered as a resilient member placed between the source of vibration and the protected body. Fig. 12a shows the simplest model of a vibro-isolating system. Fig. 12b shows the known resonant curves (displacement/velocity/acceleration transmissibility) for this system. Here  $\eta = \omega/\omega_0$ ;  $\omega$  is the frequency of vibration;  $\omega_0 = \sqrt{c/m}$  is the natural frequency of suspended body;  $c$  is the stiffness coefficient;  $m$  is the mass;  $d$  is the damping coefficient;  $A_0$  and  $A$  are the amplitudes of the sinusoidal vibration of the base and the suspended body correspondingly.

Both elasticity and damping in suspension play a significant part in the transmission of vibration. It is a known fact that for  $\omega > \sqrt{2}\omega_0$  the effectiveness of vibration isolation increases with a decrease in the stiffness of the elastic suspension while damping (friction) in the suspension reduces the effectiveness of the isolation. The dashed line in Fig. 12b corresponds to an ideal system with zero damping; the solid line corresponds to a real system with non-zero damping:  $d/(2m\omega_0) = 0.3$ . In a real system with a prescribed frequency of vibration and a prescribed natural frequency of the handle suspension the transmitted vibration can be conventionally separated into two components: 'I' determined by the elasticity of the suspension and 'II' determined by the damping (friction) in the suspension. Fig. 12b illustrates the natural limitations of vibration reduction by means of damping reduction when the second component tends to zero.

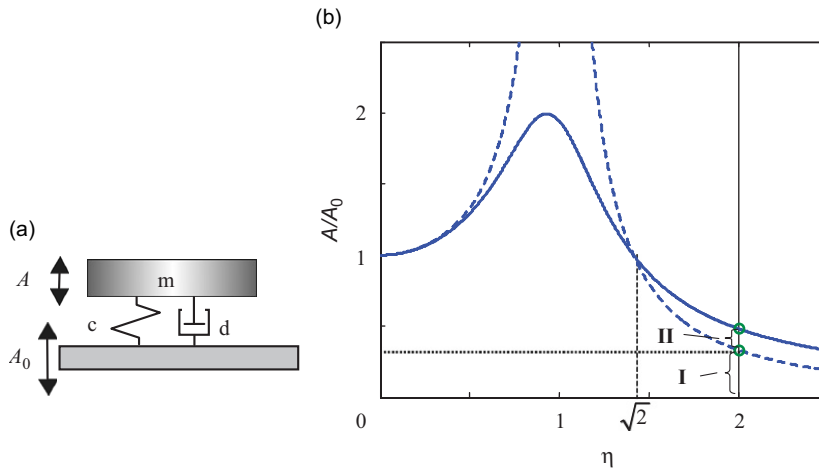


Fig. 12. Model of vibro-isolating system and resonant curves.

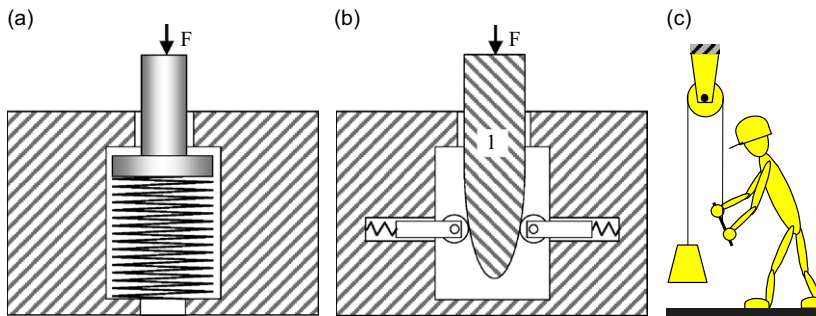


Fig. 13. Low-stiffness and zero-stiffness devices.

A more significant effect can be achieved by reducing the natural frequency of the suspended body. If the damping is negligibly small, there are no limitations for vibration reduction by means of reducing the natural frequency of the suspension, which corresponds to a reduction in component I (Fig. 12b). When passive suspension is used either increasing the mass of the suspended body or decreasing the differential stiffness of the suspension can reduce the natural frequency. Increasing the mass has obvious practical limitations. A decrease in differential stiffness poses serious technical difficulties. It is an engineering challenge to design a suspension with essential static force and zero stiffness; such a suspension has, however, a great potential in further reduction of the vibration level. Hereafter we use the term ‘zero-stiffness’ to describe a suspension that combines a prescribed static force with zero differential stiffness. The potential of such a suspension is limited only by friction.

The simplest traditional solution is to use very soft steel springs that can provide a suspension with very low, but nevertheless non-zero stiffness. Employing preloaded compressed helical springs (Fig. 13a) can, in some cases, solve a problem of high static deformation, but preloading is limited by the instability of the spring in a lateral direction. Some other mechanical devices are known which possess nonlinear force–displacement characteristics and combine high static force with low differential stiffness. One example is shown in Fig. 13b. Various profiles of the wedge 1 can provide different characteristics including one with a constant vertical force that does not change with displacement within some interval. This means that the device can have zero differential stiffness in the vertical direction. However, any increase in mechanical complexity inevitably results in increased friction, which is the other important way of vibration transmission.

The specific feature of the zero-stiffness suspension is that the suspended object is in a state of indifferent equilibrium. This should not be considered as a disadvantage for hand-held machines because the operator can easily control the position of the isolated handle within an interval of indifferent equilibrium. A point of concern could be that, possibly, the operator has no feedback, cannot ‘feel’ the machine and cannot control it because his feed force does not depend on the handle position. However, this does not complicate handling of the machine as a simple comparison with a man-operated pulley system depicted in Fig. 13c shows. If necessary, differential stiffness can be made slightly different from zero to improve feedback, but still low enough to provide good isolation. This question will be further discussed below along with experimental results. Some simple technical solutions are also possible to design semi-active suspension with frequency-dependent differential stiffness. Such a suspension can combine high stiffness at low frequencies for better controllability with low stiffness at the high frequency of vibration for good isolation. One of the possible solutions is discussed below.

A question can arise that inaccuracy in the zero-stiffness suspension constant force may destroy the necessary vibro-impact regime. Computer simulations have shown, however, that the vibro-impact regime has a very low sensitivity to the feed force. Fig. 14 demonstrates how the vibro-impact regime of the system shown in Fig. 10a changes with variation of the operator’s feed force. These results were obtained for the same parameters  $M_1, M_2, M_3, M_5, r_{12}, r_{24}$ , but for the force  $F_3$  gradually rising from 110 to 185 N. The upper graph shows the displacements of the four bodies; the curve numbers correspond to the numbers of the bodies in Fig. 9a. The lower one shows the velocity of the striker and the frequency of self-excited vibration. Frequency in the latter diagram is plotted with the dotted line.

It can be seen that the frequency of vibration rises and the impact velocity drops slightly with an increase in the feed force. However, the system demonstrates low sensitivity to the variation of feed force and the vibration remains stable when this force changes within a wide range.

It is also important for this structure that in the general case the amplitude of the balance body 2 vibration rises with a decrease in its mass, but this does not affect the handle 5. A zero-stiffness suspension has a great potential to reduce both the harmful vibration and the total mass of heavy-duty hand-held percussion tools.

The most natural and simplest zero-stiffness suspension can be achieved with a pneumatic or a hydraulic cylinder fed by a source of constant pressure (Fig. 15a). This type of zero-stiffness suspension can be naturally

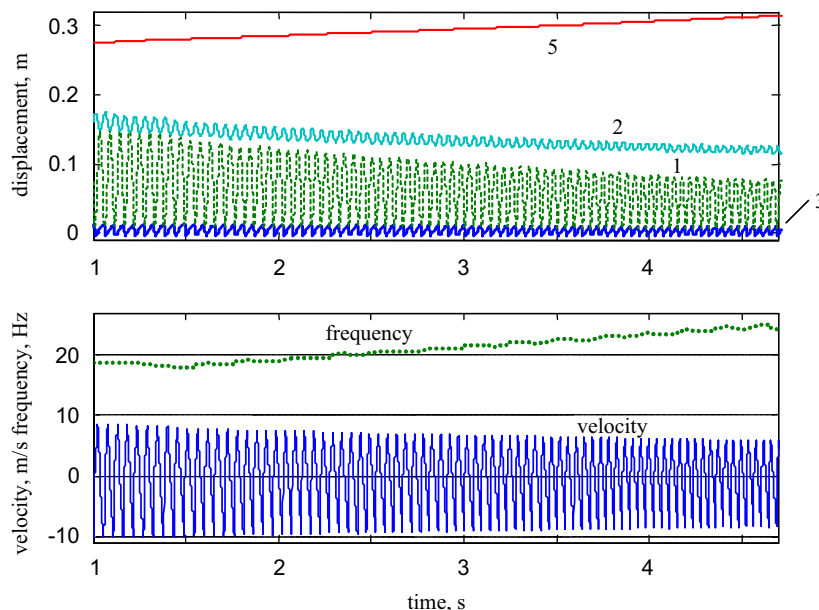


Fig. 14. Feed force variation: effect on vibro-impact regime.

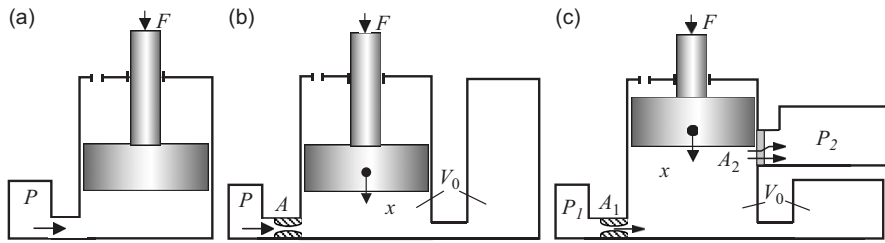


Fig. 15. Zero-stiffness pneumatic suspension.

introduced into pneumatic and hydraulic machines that are very common in manufacturing and construction. Solutions can be found for using such elements in suspension of electric machines as well.

If a source of constant pressure is available some noticeable leakage through the gap between a piston and a cylinder is admissible. Hence, there is no need to make this gap very small and as a result very low friction can be achieved. In this case a pneumatic cylinder can be very close to an ideal zero-stiffness element.

However, an ideal source of constant pressure is not always available. In practice a pressure supply can have noticeable pulsations that can reduce all advantages of zero differential stiffness. A possible solution for this case is shown in Fig. 15b which allows for filtering of the high-frequency pressure pulsations. These pulsations can be suppressed significantly by increasing the volume  $V_0$  of compressed air under the piston. However, in this case a pneumatic cylinder cannot be considered as an ideal zero-stiffness element. In fact it is more similar to the preloaded spring shown in Fig. 13a. For high-frequency vibration air below the piston can be considered as isolated from external pressure supply and adiabatic law can be applied:  $PV^\gamma = P_0V_0^\gamma$ , where  $P$  is pressure,  $V$  is volume,  $\gamma = 1.44$  for air. The differential (dynamic) stiffness is calculated as

$$c_d = \frac{dF}{dx} = S \left. \frac{dP}{dV} \frac{dV}{dx} \right|_{V=V_0} = \frac{S^2 \gamma P_0}{V_0}. \quad (11)$$

Here  $S$  is the piston area;  $P_0$  is the average pressure;  $V_0$  is total volume of air below the piston in the working position. Dynamic stiffness is inversely proportional to volume  $V_0$  and can be made as low as needed by means of increasing this volume. Also in this case the value of the gap between the cylinder and the piston is more important. If the effective area of the gap is comparable with the effective area  $A$  of the inlet orifice it affects the average pressure  $P_0$  in the cylinder.

Further development of this scheme is shown in Fig. 15c and was investigated in Ref. [9]. This pneumatic spring has a frequency-dependent dynamic stiffness. The effective area of the outlet orifice depends on the piston position:  $A_2 = A_2(x)$ . If the piston vibrates with a high frequency, the average pressure  $P_0$  in the cylinder depends only on the average position  $x_0$  of the vibrating piston and is given by

$$P_0 = \frac{P_1 A_1 + P_2 A_2(x_0)}{A_1 + A_2(x_0)}. \quad (12)$$

This expression determines the static stiffness of the pneumatic spring  $c_{st} = S(dP_0(x_0)/(dx_0))$ , which does not depend on the volume  $V_0$ . As opposed to static stiffness, the dynamic stiffness, which determines the transmission of the vibration, is described by Eq. (11) and can be made very small by increasing the volume  $V_0$ . This combination of high static stiffness and low dynamic stiffness is ideal for hand-held machines as it enables an operator to have good “feel” of the machine while being protected from high-frequency vibration.

In hydraulic tools the scheme shown in Fig. 15a can be applied without any alterations if a source of constant hydraulic pressure is available. Otherwise, in the case of a pulsating pressure source the scheme shown in Fig. 15b can be used with an added gas accumulator as Fig. 16 shows. The scheme shown in Fig. 15c can be adapted the same way.

In order to make a simple comparison between the hydraulic and pneumatic systems the expression (11) for dynamic stiffness can be rewritten in the following form:

$$c_d = \gamma F^2 \frac{1}{P_0 V_0}, \quad (13)$$

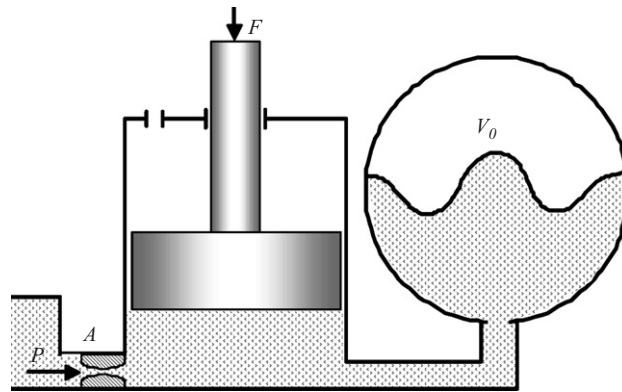


Fig. 16. Hydro-pneumatic suspension.

where  $F = P_0 S$  is the feed force. It is seen now that for the prescribed feed force  $F$  the same low value of dynamic stiffness  $c_d$  can be achieved in a hydraulic system with a smaller volume  $V_0$  of compressed air than in a pneumatic system. This is because the working pressure  $P_0$  in hydraulic systems is usually much higher than in pneumatic systems.

As dynamic stiffness can easily be made very low when using hydraulic or pneumatic devices, more attention should be paid to friction (damping) that becomes the governing factor in transmission of vibration. Traditional bellows and modern rubber-metal analogues can be considered as a substitute to cylinders in some cases with the aim of reducing friction in the zero-stiffness suspension.

The solution shown in Fig. 16 has been recently patented by JCB [10]. It was successfully tested on a commercially available heavy-duty hand-held hydraulic breaker. This breaker is usually used with a simple constant flow power pack. Reciprocating motion of the striking piston driven by the constant flow of hydraulic fluid results in high pulsations of pressure. This prevents the use of the simplest solution shown in Fig. 15a. In the existing design of the spring suspended rotating handles the spring suspension was replaced by the hydro-pneumatic suspension as in Fig. 16. In the tests the RMS vibration  $a_c$  off the casing and  $a_h$  of the handle have been measured.

Initial experiments have shown that vibration of the casing slightly rose as a result of lower dumping on the operator's side. However, the new suspension allowed for improving the vibration suppression ratio  $a_h/a_c$  to 0.20 as against 0.43 in the original breaker. As a result, the original handle vibration  $4.94 \text{ m/s}^2$  was reduced to  $3.00 \text{ m/s}^2$ . There is a room for further reduction of vibration by modification of the breaker handle design.

These experiments have also shown that an operator does not have any serious difficulties while operating a breaker with zero-stiffness suspension, although the feel is slightly different as compared to operating a breaker with spring-suspended handles.

## 5. Conclusions

It is possible to synthesise hand-held percussion machine as a structure with an intensive vibro-impact process on one side and a vibration-free handle on the other side. The simplest three-body system with one vibration-free body needs higher operator's feed force than conventional machines. In the four-body structure, however, this can be achieved without increase in the feed force. Feasibility of this solution was proved by computer simulations and experiments on the modified industrial machine. This approach has a great potential of reduction in vibration transmitted to the operator. In practice this reduction is limited only by friction in the zero-stiffness suspension of the handle.

## Acknowledgements

Authors thank the management and employees of JCB for support of this project and fruitful collaboration.

## References

- [1] V.I. Babitsky, Hand-held percussion machine as discrete non-linear converter, *Journal of Sound and Vibration* 214 (1998) 165–182 (Erratum 222(5) (1999)).
- [2] G. Bisutti, Power tool, European Patent EP1 005 403 B1, 2002.
- [3] J.F. Nikitin, D.J. Nikitin, N.A. Rykov, I.L. Terekhov, Pneumatic tool, United States Patent number 4,402,369, 1983.
- [4] V.I. Babitsky, Appendix I: Simulation of Impact in Viscoelastic Limiter. *Theory of Vibro-Impact Systems and Applications*, Springer, Berlin, 1998.
- [5] V.I. Babitsky, A.M. Veprik, Universal bumpered vibration isolator for severe environment, *Journal of Sound and Vibration* 218 (1998) 269–292.
- [6] Atlas Copco manual, fourth ed., Atlas Copco, 1982, pp. 185–186.
- [7] S. Anderson, *RDR-36-a New Chipping Hammer with Unique Design*, Atlas Copco, Stockholm, 1976.
- [8] P. Alabuzhev, A. Gritchin, L. Kim, G. Migirenko, V. Chon, P. Stepanov, *Vibration Protecting and Measuring Systems with Quasi-Zero Stiffness*, Hemisphere Publishing Co., New York, 1989.
- [9] R. Palej, S. Piotrowsky, M. Stojek, Mechanical properties of an active pneumatic spring, *Journal of Sound and Vibration* 168 (1993) 299–306.
- [10] A.A. Malkin, I. Sokolov, V. Babitsky, Percussion power tool apparatus with shock absorbing piston arrangement, UK Patent GB2421466, 2006.